

Four-wheel Anti-lock Braking System with Road Condition Detection Module

Jinhong Sun.¹ Ka Wai Eric Cheng.²

^{1,2}Power Electronics Research Centre, The Hong Kong Polytechnic University, Hong Kong
E-mail: jinhong.sun@connect.polyu.hk¹ eric-cheng.cheng@polyu.edu.hk²

Abstract –The anti-lock braking system (ABS) designed based on the wheel slip control (WSC) method becomes more and more popular, especially after the in-wheel technology (IWT) is developed. With the help of IWT, a four-wheel braking control algorithm based on the robust fuzzy sliding mode WSC method is proposed. It mainly focuses on improving the robustness of the braking performance under complex road conditions, the steady-state achievement, and the reduction of the tracking error. The novelty is that the road condition detection module is added, which provides the road conditions to the ABS controller through acceleration training. This proposed four-wheel ABS is validated with enough robustness in dealing with complex road conditions through the simulation.

Keywords - anti-lock braking system, wheel slip control, in-wheel motor, road condition detection module

I. INTRODUCTION

Nowadays, many control strategies have been used to develop the anti-lock braking controller, which mainly including two types: the wheel acceleration-based control method and the wheel slip-based control method. The wheel acceleration-based one indirectly controls the wheel slip by controlling the wheel's deceleration or acceleration through brake pressure from a brake actuator. And the control algorithm with a logic threshold acceleration was developed and widely utilized in the ABS manufacturing industry [1]. However, this kind of ABS controller has some drawbacks on robust control as it largely depends on the experience of pre-setting the control thresholds [2]. Therefore, the wheel slip-based control method becomes more and more popular, especially with the development of IWT [3, 4]. Many control algorithms have been used to improve the control performance, such as the optimal wheel slip-based localization through the use of the proportional-integral-derivative (PID) method, the fuzzy method, and the neural network method [5].

Even though the hydraulic-based brake actuator is widely used in the automobile industry, the latest automotive electrification and automation trends still have some new challenges [6] with the optimization of WSC-based ABS. Despite the significant progress of ABS that has taken place over the last few years, with the current high demand in autonomous driving, smart control, and electric vehicle, new issues that constitute an open topic for research emerge. Among them, when braking on complex roads, the controller's robustness, steady-state performance and accuracy of tracking error need to be further studied, especially for designing a vehicle's four-wheel ABS. Different research activities are focused on the electro-hydraulic (EHB) brakes, and some research activities have been successfully implemented in the lab for a variety of EVs [2, 7].

Furthermore, another set-back is that modern and future generations of electric vehicles require the anti-lock braking controller to provide sufficient robustness for various road conditions. Recently, many control algorithms are used to build the required braking controller, such as the linear one: PID control [8], fuzzy logic control [9], and the nonlinear one: the sliding mode [10]. As the in-wheel motor is directly fixed inside the wheel, the proposed nonlinear anti-lock braking controller can adjust the braking force quickly to deal with the disturbances [11]. Generally, the significant difficulty involved in the design of the ABS is that the control performance depends strongly on the knowledge of the wheel and road characteristics, and the optimal wheel slip varies significantly with the road conditions. Besides, the real-time wheel slip depends on the wheel speed measured by the speed sensor, and vehicle velocity estimated by vehicle model; thus, the wheel slip is chosen as the direct control object of most anti-lock braking controllers [12]. The wheel speed is changed by adjusting the brake torque, thus, the real-time wheel slip is controlled within the expected range based on the road conditions [13].

II. ANALYSIS OF THE VEHICLE DYNAMICS

Table I shows the parameters of the established vehicle model, where, ($i = 1, 2, 3, 4$) represent the left-front, right-front-right, left-rear, right-rear-right wheels, respectively. Other parameters are given in Table 1.

Table 1: Parameters of the ABS model

Sign	Description
μ_{r_i}	Rolling friction coefficient
$M(kg)$	Full mass of the vehicle
$R_w = 0.2768(m)$	Radius of the single wheel
$m_w = 12(kg)$	Single wheel weight
$J = 0.92(kg/m^2)$	Inertia of the single wheel
$\rho = 1.25(kg/m^3)$	Air density
$C_{air} = 0.23$	Air resistance coefficient
$A_{air} = 2.37(m^2)$	Air resistance area
$F_{br} = 11(kN)$	Rated braking force

A. Dynamical analyses of vehicle

The dynamic characteristics: the single wheel and the whole vehicle are formulated in (1), respectively. Actually, there have some forces that effect the control accuracy, such as the drag force from air F_{air} and the resistant force from the wheel rolling friction F_r . Therefore,

$$\begin{cases} \frac{d\omega_i}{dt} = \mathbf{A} = \frac{R_w}{J} \mathbf{F}_f - \frac{1}{J} \mathbf{T} \\ \frac{dv_{v_x}}{dt} = \dot{v}_{v_x} = -\frac{1}{M} [\mathbf{F}_f^T \mathbf{I} + \mathbf{F}_r^T (\mathbf{I} - \mathbf{S}_1) + F_{air}] \end{cases} \quad (1)$$

Here, \mathbf{A} is a matrix of ω_i , \mathbf{S}_1 and \mathbf{T} are constructed by instant wheel data, describe λ_i and T_{b_i} , respectively.

$$\mathbf{A} = \begin{bmatrix} \dot{\omega}_1 \\ \dot{\omega}_2 \\ \dot{\omega}_3 \\ \dot{\omega}_4 \end{bmatrix}, \quad \mathbf{S}_1 = \begin{bmatrix} \lambda_1 \\ \lambda_2 \\ \lambda_3 \\ \lambda_4 \end{bmatrix}, \quad \mathbf{T} = \begin{bmatrix} T_{b1} \\ T_{b2} \\ T_{b3} \\ T_{b4} \end{bmatrix} \quad (2)$$

Besides, \mathbf{F}_f and \mathbf{F}_r represent F_{f_i} and F_{r_i} , encompassing the real-time data at each sampling time for every single wheel (FL, FR, RL, and RR), respectively.

$$\mathbf{I} = \begin{bmatrix} 1 \\ 1 \\ 1 \\ 1 \end{bmatrix}, \quad \mathbf{F}_f = \begin{bmatrix} F_{f1} \\ F_{f2} \\ F_{f3} \\ F_{f4} \end{bmatrix}, \quad \mathbf{F}_r = \begin{bmatrix} F_{r1} \\ F_{r2} \\ F_{r3} \\ F_{r4} \end{bmatrix} \quad (3)$$

Finally, the description of the forces mentioned above is summarized and shown in (4), where μ_i means the friction coefficient, and β_i stands for the force weight of each wheel.

$$\begin{cases} F_{f_i} = \frac{\mu_i \times M \times g}{\beta_i} \\ F_{r_i} = \frac{\mu_{r_i} \times M \times g}{\beta_i} \\ J = m_w \times R_w^2 \\ F_{air} = 0.5 \times \rho \times C_{air} \times A_{air} \times v_{v_x}^2 \end{cases} \quad (4)$$

B. Description of the wheel slip

According to the magic formula mentioned by Pacejka [13], which is used in MATLAB to simulate the braking operation and widely used in many literatures, four kinds of road conditions are demonstrated in Fig. 1. For the $\mu - \lambda$ friction curve shown in this figure, the dry, wet, snow, and icy roads can be divided based on the mathematical theory.

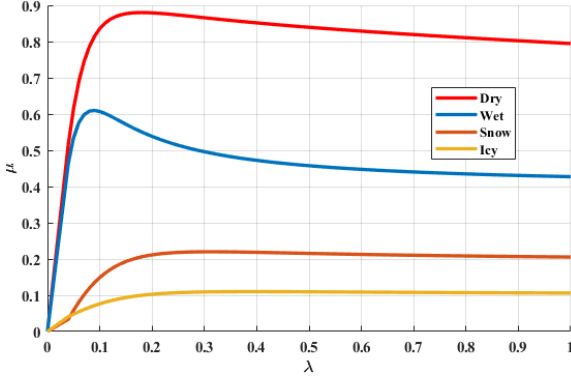


Fig.1 Four types of road conditions

For the wheel slip control method, the design target is the real-time wheel slip. Thus, the wheel slip dynamics can be obtained below,

$$\begin{cases} \lambda_i = \frac{v_{v_x} - \omega_i R_w}{v_{v_x}} \\ \frac{d\lambda_i}{dt} = \dot{\lambda}_i = -\frac{\dot{\omega}_i R_w - \dot{v}_{v_x}(1 - \lambda_i)}{v_{v_x}} \end{cases} \quad (5)$$

Define $(\lambda_i, \dot{\lambda}_i)$ as the wheel slip characteristics, and S_2 to represent the $\dot{\lambda}_i$ characteristic. Therefore, (5) can be re-defined in (6).

$$\begin{cases} \mathbf{S}_1 = \mathbf{I} - \frac{R_w}{v_{v_x}} \mathbf{W} \\ \mathbf{S}_2 = -\frac{R_w}{v_{v_x}} \mathbf{A} + \frac{\dot{v}_{v_x}}{v_{v_x}} (\mathbf{I} - \mathbf{S}_1) \end{cases} \quad (6)$$

Here, \mathbf{W} stands for four wheels' ω_i at each sampling time, which can be measured through the wheel angular speed sensor.

$$\mathbf{W} = \begin{bmatrix} \omega_1 \\ \omega_2 \\ \omega_3 \\ \omega_4 \end{bmatrix}, \quad \mathbf{S}_2 = \begin{bmatrix} \dot{\lambda}_1 \\ \dot{\lambda}_2 \\ \dot{\lambda}_3 \\ \dot{\lambda}_4 \end{bmatrix} \quad (7)$$

III. DESCRIPTION OF THE CONTROL METHOD

A. Road condition detection module

Fig. reveals the control detail of the proposed all-electric ABS. After a series of signal processing, the anti-lock braking controller's output signals and the associated braking torque requirement are transmitted back to the ECU and further transmitted by the ECU to the power controller to control the speed of the braking motor (also considered as the braking actuator).

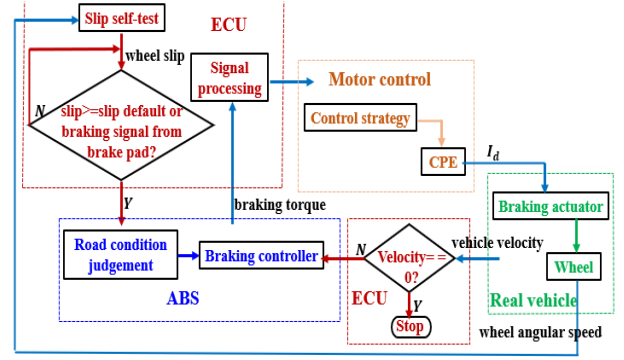
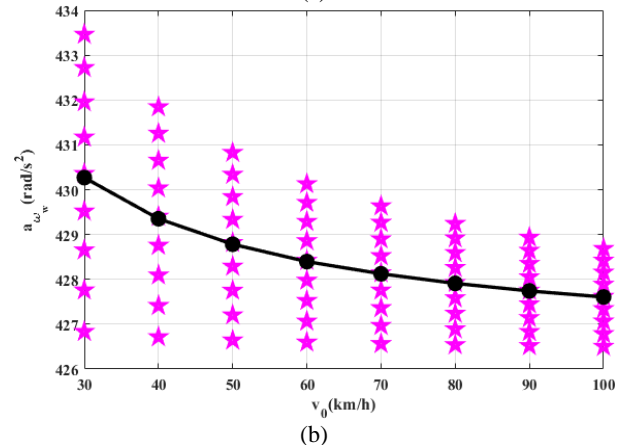
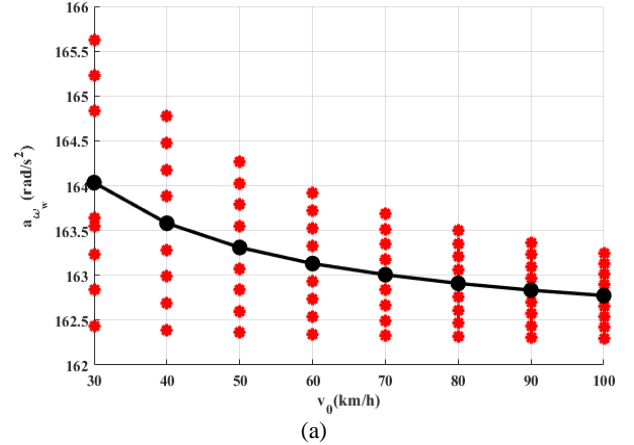


Fig.2 Control flow of the all-electric ABS

For the road condition detection module, the angular acceleration of every wheel is calculated at each sampling time under the initial braking force F_b during the calculation period Δt . Assume that, $F_b = 0.4 \times F_{b_r}$, and F_{b_r} is the rated braking force equals to $11kN$. F_b is applied at $t = 0s$, and the angular wheel acceleration a_{ω} must be measured in the time window from t_1 to t_n with the specified sampling frequency $f = 1kHz$. Define a_{ω_m} to represent the average of a_{ω} , thus,



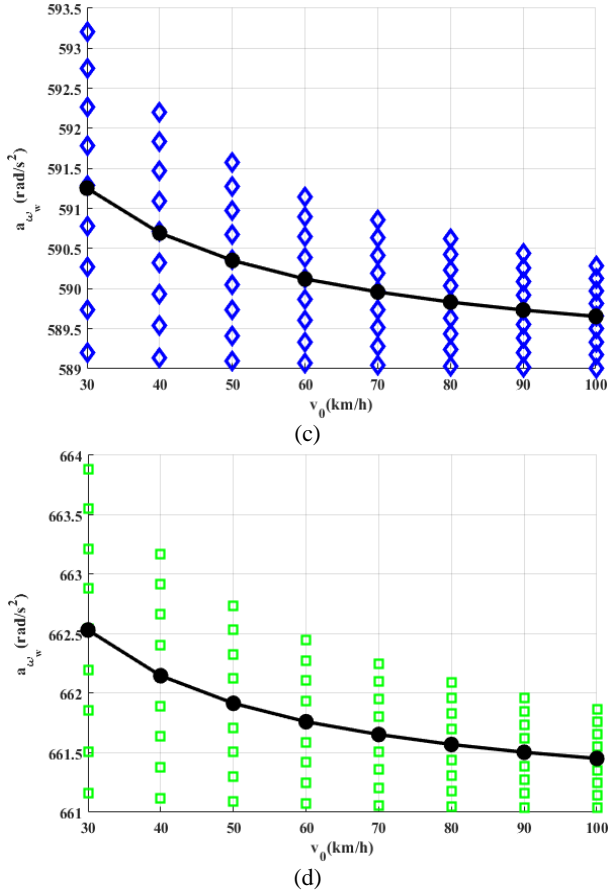


Fig.3 a_{ω_m} of the four types of road conditions (a) dry (b) wet (c) snow (d) icy

The acceleration indicators of the four typical roads are shown in Fig.3, and road condition judgement rules can be summarized below,

- If $164 \text{ rad/s}^2 \leq a_{\omega} < 164 \text{ rad/s}^2$, the wheel is braking on the dry road, and the optimal wheel slip λ_0 , the adhesion friction coefficient μ of the real road are in the dry condition curve shown in Fig.1.
- If $427 \text{ rad/s}^2 \leq a_{\omega} < 430 \text{ rad/s}^2$, the wheel is braking on the wet road, and λ_0 and μ are in wet condition curve shown in Fig.1.
- If $590 \text{ rad/s}^2 \leq a_{\omega} < 591 \text{ rad/s}^2$, the wheel is braking on the snow road, and λ_0 and μ are in snow condition curve shown in Fig.1.
- If $661 \text{ rad/s}^2 \leq a_{\omega} < 663 \text{ rad/s}^2$, the wheel is braking on the icy road, and λ_0 and μ are in icy condition curve shown in Fig.1.

The angular acceleration speed is considered as the preliminary basis for determining the road conditions. Next, λ_0 and μ that generated by the above module are put into the braking controller.

B. Wheel slip

As well known, the operating principle can be concluded that through adjusting the braking torque to control the wheel speed, then affect the wheel slip. Based on (1), (4), and (5), the dynamic of wheel slip can be expressed in (8).

$$\dot{\lambda}_i = -\frac{1}{v_{v_x}} \{ [\mu_i g + \mu_{r_i} g (1 - \lambda_i)] (1 - \lambda_i) \} + \frac{T_{bw_i}}{v_{v_x} m_w R_w} \quad (8)$$

The control target of designed ABS can be obtained,

$$bT_{b_i} = \dot{\lambda}_i + \frac{1}{v_{v_x}} \left[\frac{F_{f_i} \beta_i (1 - \lambda_i)}{M} + \frac{F_{r_i} (1 - \lambda_i)}{m_w} + \frac{F_{air} (1 - \lambda_i)}{M} \right] \quad (9)$$

C. Fuzzy sliding mode control

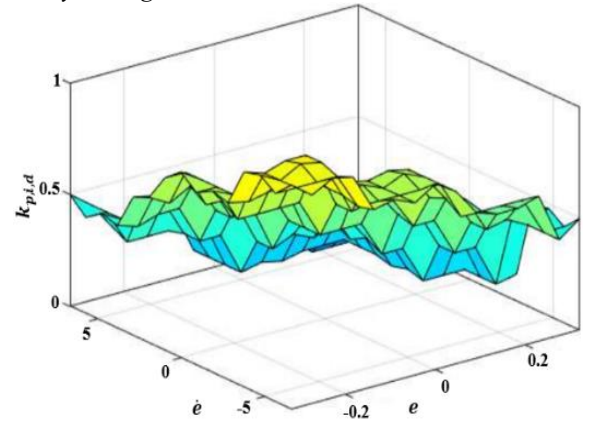


Fig.4 Fis of fuzzy controller's k_p , k_i and k_d

The algorithm of the anti-lock braking controller is built based on the fuzzy sliding mode WSC. The fuzzy function can easily incorporate the control experiences into the fuzzy controller through fuzzy rules, which reduces the difficulty of designing the controller. Define the error characteristic $e_i = \lambda_{0_i} - \lambda_i$, and its time derivative can be expressed as $\dot{e} = \frac{de_i}{dt} = \dot{\lambda}_{0_i} - \dot{\lambda}_i$. According to fuzzy rules of the fuzzy controller, PID variables can be yielded in Fig.4.

Then, variables of the fuzzy PID controller also considered as the input parameters of the fuzzy sliding mode controller can be obtained in (10). Where, k_{p,i,d_0} means the initial correction value of k_{p_0} , k_{i_0} , k_{d_0} .

$$K_{P,I,D_i} = k_{p,i,d}(e_i, \dot{e}_i) \times k_{p,i,d_0} \quad (10)$$

For the sliding mode controller, the sliding surface and its time derivatives are set as,

$$\begin{cases} s = e + K_{P_i} \int e + K_{I_i} \iint e + K_{D_i} \dot{e} \\ \dot{s} = \dot{e} + K_{P_i} e + K_{I_i} \int e + K_{D_i} \dot{e} \end{cases} \quad (11)$$

Based on the Lyapunov principle: $V = \frac{1}{2} s^2 \Rightarrow \dot{V} = s\dot{s}$, FIS rules of this fuzzy sliding controller can be obtained and demonstrated in Fig.5.

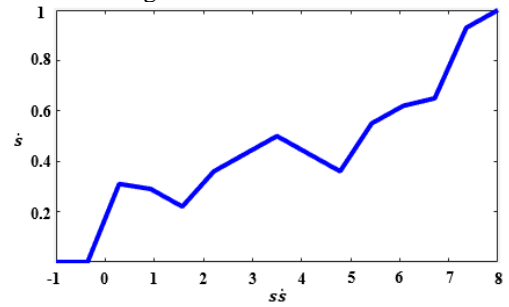
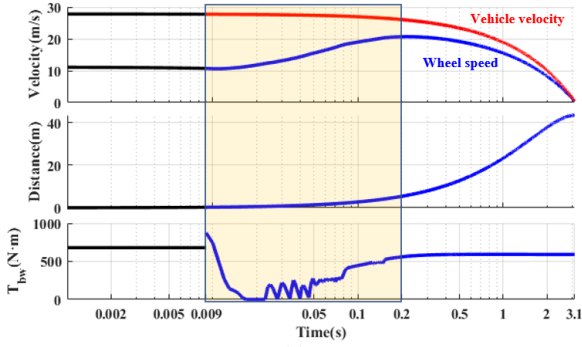


Fig.5 Fis of the sliding surface characteristic s and \dot{s}

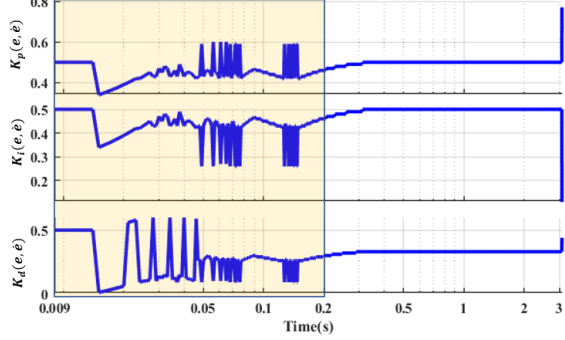
IV. SIMULATION RESULTS

The vehicle model has been built based on the vehicle dynamics and the ABS control method, in which the straight-line case is chosen as the braking situation. Initial wheel slip λ_0 is set with a large value and are all done with the initial vehicle velocity $v_0 = 100 \text{ km/h}$.

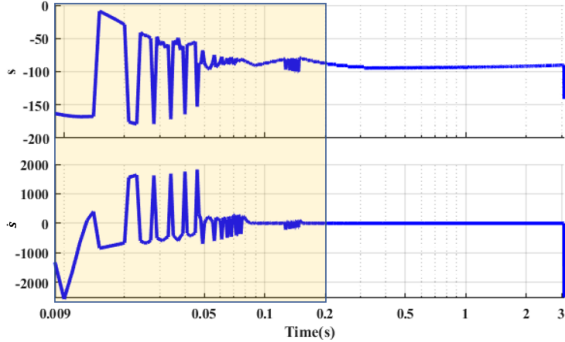
Fig.6 shows the details of the vehicle braking on dry road conditions under the control of the four-wheel ABS controller. The whole adjustment of braking torque and velocities and the stop distance trend are given in Fig.6 (a). Parameters of the robust controller are shown in Fig.6 (b) and Fig.6 (c).



(a)

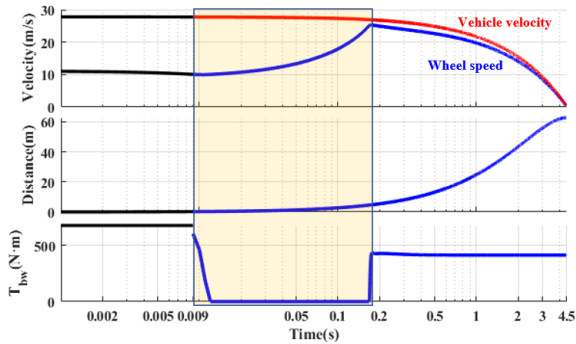


(b)

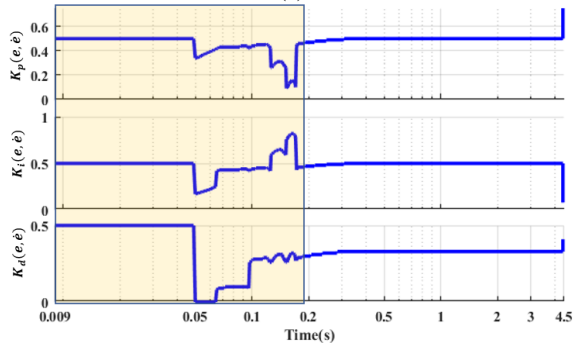


(c)

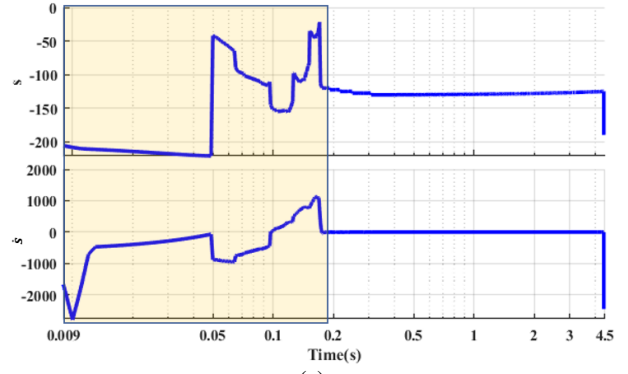
Fig.6 Control performance on dry road



(a)



(b)



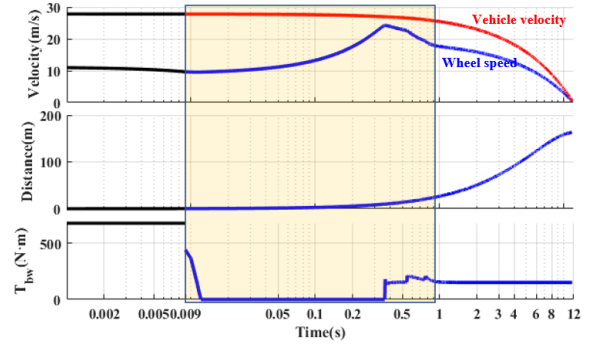
(c)

Fig.7 Control performance on wet road

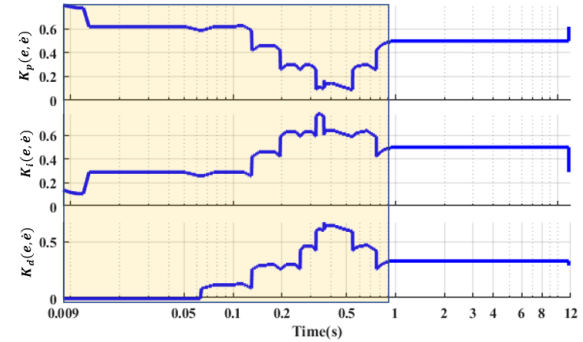
During $[0, 0.009]$ s, the vehicle is braking with the fixed braking force, and the road condition detection module operates to obtain the road information. Then these data can be transferred into the ABS controller, and ABS starts. The yellow shadow area represents the ABS control range with an obvious adjust function, and the smaller the range, the better the braking convergence. For dry roads, the braking stabilization time is controlled at about 0.2s.

Similarly, for the wet road condition, the vehicle still starts braking under the fixed braking force during 0.09s. After that, ABS operates to adjust the braking torque. Almost before 0.18s, the adjustment control reaches stable.

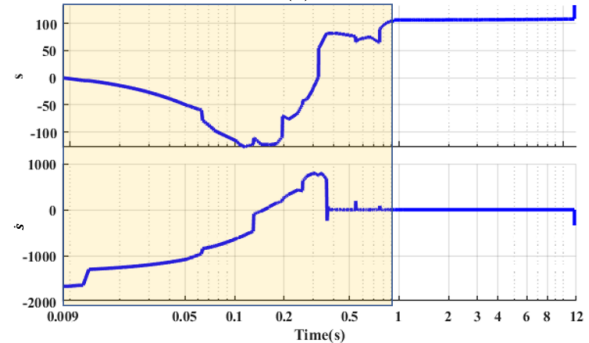
Fig.8 and Fig.9 show the control performance details on snow and icy roads, respectively.



(a)



(b)



(c)

Fig.8 Control performance on snow road

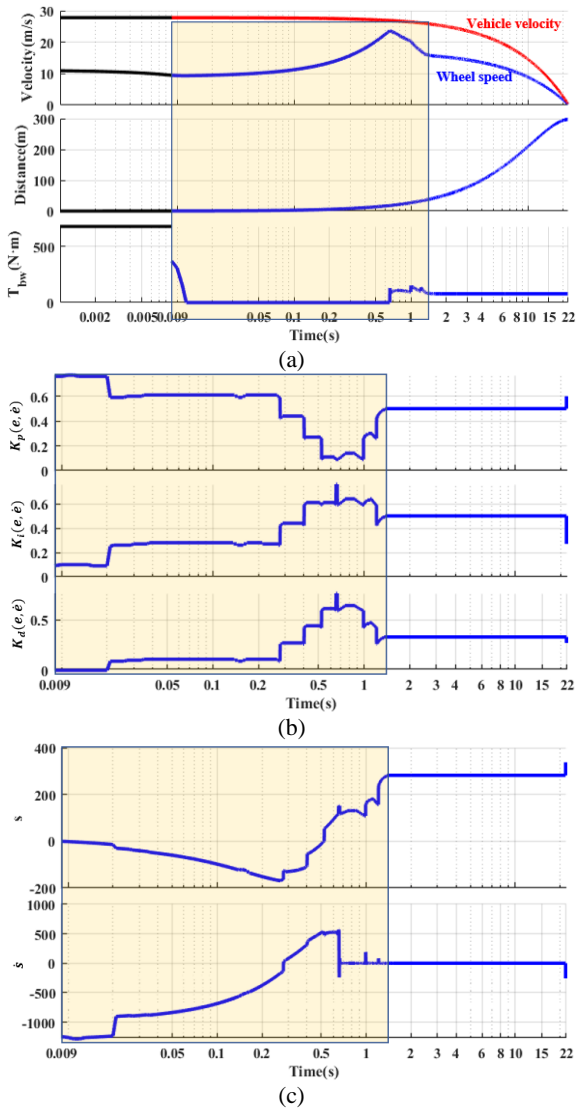


Fig.9 Control performance on icy road

For these two kinds of road conditions, the control performance is quite similar; however, the time to reach control stability has increased.

IV. CONCLUSION

In this paper, the anti-lock braking system with a road condition detection module for the four-wheel model is proposed, which is established based on the fuzzy sliding mode wheel slip control method. This proposed ABS controller is validated with enough robustness to deal with braking control on different road conditions through simulation. The road condition detection module works on providing road information to the ABS controller. This function improves the braking control accuracy and

maintains the braking control achieving a stable state as soon as possible.

REFERENCES

- [1] X. D. Xue, K. W. E. Cheng, T. W. Ng and N. C. Cheung, "Multi-Objective Optimization Design of In-Wheel Switched Reluctance Motors in Electric Vehicles," *IEEE Transactions on Industrial Electronics*, vol. 57, no. 9, pp. 2980-2987, Sept. 2010.
- [2] D. Savitski, D. Schleinin, V. Ivanov and K. Augsborg, "Robust Continuous Wheel Slip Control With Reference Adaptation: Application to the Brake System With Decoupled Architecture," *IEEE Transactions on Industrial Informatics*, vol. 14, no. 9, pp. 4212-4223, Sept. 2018.
- [3] H. Jing, Z. Liu and H. Chen, "A Switched Control Strategy for Antilock Braking System With On/Off Valves," *IEEE Transactions on Vehicular Technology*, vol. 60, no. 4, pp. 1470-1484, May 2011.
- [4] J. J. Castillo, J. A. Cabrera, A. J. Guerra and A. Simón, "A Novel Electrohydraulic Brake System With Tire-Road Friction Estimation and Continuous Brake Pressure Control," *IEEE Transactions on Industrial Electronics*, vol. 63, no. 3, pp. 1863-1875, March 2016.
- [5] Y. Chen, C. Tu and C. Lin, "Integrated electromagnetic braking/driving control of electric vehicles using fuzzy inference," *IET Electric Power Applications*, vol. 13, no. 7, pp. 1014-1021, July 2019.
- [6] D. Tavernini *et al.*, "An Explicit Nonlinear Model Predictive ABS Controller for Electro-Hydraulic Braking Systems," *IEEE Transactions on Industrial Electronics*, vol. 67, no. 5, pp. 3990-4001, May 2020.
- [7] A. Patil, D. Ginoya, P. D. Shendge and S. B. Phadke, "Uncertainty-Estimation-Based Approach to Antilock Braking Systems," *IEEE Transactions on Vehicular Technology*, vol. 65, no. 3, pp. 1171-1185, March 2016.
- [8] H. Sun, J. Yan, Y. Qu and J. Ren, "Sensor fault-tolerant observer applied in UAV anti-skid braking control under control input constraint," *Journal of Systems Engineering and Electronics*, vol. 28, no. 1, pp. 126-136, Feb. 2017.
- [9] W. Sun, J. Zhang and Z. Liu, "Two-Time-Scale Redesign for Antilock Braking Systems of Ground Vehicles," *IEEE Transactions on Industrial Electronics*, vol. 66, no. 6, pp. 4577-4586, June 2019.
- [10] Y. Wang, H. Fujimoto and S. Hara, "Driving Force Distribution and Control for EV With Four In-Wheel Motors: A Case Study of Acceleration on Split-Friction Surfaces," *IEEE Transactions on Industrial Electronics*, vol. 64, no. 4, pp. 3380-3388, April 2017.
- [11] X. Wu, M. Zhang and M. Xu, "Active Tracking Control for Steer-by-Wire System With Disturbance Observer," *IEEE Transactions on Vehicular Technology*, vol. 68, no. 6, pp. 5483-5493, June 2019.
- [12] J. Ni, J. Hu and C. Xiang, "Envelope Control for Four-Wheel Independently Actuated Autonomous Ground Vehicle Through AFS/DYC Integrated Control," *IEEE Transactions on Vehicular Technology*, vol. 66, no. 11, pp. 9712-9726, Nov. 2017.
- [13] J.H.Sun, X.D.Xue, K.W.E.Cheng, "Fuzzy Sliding Mode Wheel Slip Control for Smart Vehicle Anti-lock Braking System," *Energies*, vol. 12, no. 13, pp. 2501, 2019